

# Frequency Offset Estimation for MB-OFDM-based UWB Systems

Yinghui Li, Trent Jacobs, and Hlaing Minn

Department of Electrical Engineering, University of Texas at Dallas

{yx1044000, taj016000, hlaing.minn}@utdallas.edu.

**Abstract**—We address low-complexity, highly-accurate frequency offset estimation for MB-OFDM-based UWB systems. We discuss unique characteristics of the MB-OFDM systems, namely, different carrier frequency offsets, different channel responses, different channel energies, and different preamble structures in different frequency bands. Utilizing them, we develop frequency offset estimators based on the best linear unbiased estimation principle. If compared to the conventional estimators using correlation and averaging, our proposed methods achieve better estimation performance for all preamble patterns and the improvement is more significant for the preamble patterns 3 and 4 of the MB-OFDM system in [2].

## I. INTRODUCTION

The Multi-Band Orthogonal Frequency Division Multiplexing (MB-OFDM) systems have attracted much research attention and have been proposed for the IEEE 802.15.3a ultra-wide band (UWB) standard [1]- [3]. The very high data rate (480 Mbps and beyond) capability of the 802.15.3a technology would provide a very compelling cable-replacement wireless technology. At the same time, the high frequency bands as well as the application of OFDM technology demand highly accurate frequency offset estimation since frequency offset causes a loss of orthogonality among the subcarriers which introduces inter sub-carrier interference and degrades the error performance significantly.

In the MB-OFDM proposal for the IEEE 802.15.3a, a preamble is used to aid receiver algorithms related to timing and frequency synchronization, and channel estimation. There are several preamble-based frequency offset estimators (e.g., [4]- [9]) in the research literature. However, we have not observed frequency offset estimators derived for the MB-OFDM systems. In MB-OFDM systems, the oscillator frequency offset causes different carrier frequency offsets for the different bands. The channel frequency responses and the channel energies for the different bands are different as well. The frequency hopping of the MB-OFDM system results in different preamble structures for some of the frequency bands. These unique characteristics of the MB-OFDM systems motivate us to develop highly-accurate, low complexity frequency offset estimators based on the best linear unbiased estimation (BLUE) principle. Our proposed estimators incorporate these characteristics and achieve better performance over the conventional method using correlation and averaging. Our results also show that different preamble patterns give different mean-square error (MSE) performances and the improvement of our

methods over the conventional method is more significant for the preamble patterns 3 and 4 of [2].

## II. SIGNAL MODEL

In the MB-OFDM-based UWB system [2], the carrier frequency is hopped within a pre-defined set of carrier frequencies  $\{f_q\}$  (corresponding to disjoint frequency bands) from symbol to symbol according to a time-frequency code. Zero-padded guard intervals ( $N_{\text{pre}}$  prefix and  $N_{\text{suf}}$  suffix zero samples;  $N_g = N_{\text{pre}} + N_{\text{suf}}$ ;  $M_0 = N + N_g$ ) are used instead of the conventional cyclic prefix guard interval. The low-pass-equivalent time-domain training samples  $\{s_q(k = mM_0 + N_{\text{pre}} + n)\}$  (sampled at  $N/T = 1/T_s$ ,  $N$  times the sub-carrier spacing) transmitted during the  $m$ -th symbol interval in the  $q$ -th frequency band are generated by taking the  $N$ -point inverse fast Fourier transform (IFFT $_N$ ) of the sub-carrier symbols  $\{C_{q,m}(l)\}$  (zeros for null sub-carriers; all zeros if no symbols are transmitted in the  $q$ -th band during the  $m$ -th interval) and inserting zero guard-samples as<sup>1</sup>

$$s_q(k) = \begin{cases} \frac{1}{N} \sum_{l=0}^{N-1} C_{q,m}(l) e^{j2\pi lk/N}, & 0 \leq n \leq N-1 \\ 0, & -N_{\text{pre}} \leq n < 0; N \leq n < N + N_{\text{suf}}. \end{cases} \quad (1)$$

The IEEE 802.15.3a UWB RF channel model described in [11] is given by

$$h_{\text{RF}}(t) = X \sum_{l=0}^{L_h} \sum_{k=0}^K \alpha_{k,l} \delta(t - T_l - \tau_{k,l}) \quad (2)$$

where  $\alpha_{k,l}$ ,  $T_l$ ,  $\tau_{k,l}$ , and  $X$  are random variables representing the multipath gain coefficients, the delay of the  $l$ -th cluster, the delay (relative to the  $l$ -th cluster arrival time) of the  $k$ -th multipath component of the  $l$ -th cluster, and the log-normal shadowing, respectively. Details of this channel model are referred to [11]. In this paper, we consider a low-pass-equivalent system which absorbs the carrier-frequency hopping into the channel impulse response (CIR). The sample-spaced low-pass-equivalent CIR for the  $q$ -th band is given by

$$h_q(n) = X \sum_{l=0}^{L_h} \sum_{k=0}^K \alpha_{k,l} e^{-j2\pi f_q(T_l + \tau_{k,l})} p(nT_s - T_l - \tau_{k,l} - t_0) \quad (3)$$

where  $p(t)$  is the combined transmit and receive filter impulse response and  $t_0$  is a delay for the causality. From (3), we can observe that the channel energies in different bands are different.

For the (mandatory) Mode-1 of the MB-OFDM system [2], the carrier frequency synthesizer using just one oscillator as described in [3] is shown in Fig. 1. Note that the normalized

<sup>1</sup>Note that for each band, we use the corresponding low-pass-equivalent system. The effects of different carrier frequencies are embedded in the low-pass-equivalent channels.

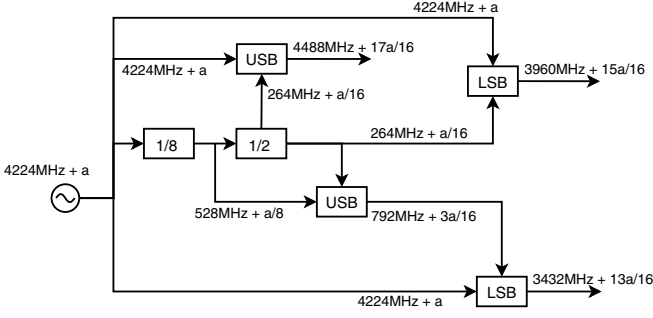


Fig. 1. The carrier frequency synthesizer for Mode-1 of [2]. (Also shown are the different carrier frequency offsets for the different carrier frequencies.)

OFO  $v$  causes different CFOs  $\{v_q\}$  for the different bands as illustrated in Fig. 1 and their relationship<sup>2</sup> is given by

$$v_q = b_q v, \quad q = 1, 2, 3 \quad (4)$$

$$[b_1, b_2, b_3] = \left[ \frac{13}{16}, \frac{15}{16}, \frac{17}{16} \right]. \quad (5)$$

The MB-OFDM system from [2] has 4 different preamble patterns (for 4 pico-nets), each associated with a different time-frequency code. Each preamble pattern is constructed by successively repeating a time-domain preamble sequence (symbol) over 21 periods as  $\{PS_0, PS_1, \dots, PS_{20}\}$ . The preambles in each of the three different bands are shown in Fig. 2. The preamble patterns 1 and 2 (or, 3 and 4) have the same structure except the ordering of the carrier frequencies. But the preamble pattern 3 or 4 has a structure different from the pattern 1 or 2.

We assume that the timing synchronization eliminates inter-symbol-interference. Define  $\{t_l^q\} = \{t_l^q(i) : i = 0, \dots, N-1; l = 1, \dots, L_q\}$  where  $\{t_l^q(i) : i = 0, 1, \dots, N-1\}$  denotes the time-domain sample index set corresponding to the  $l$ -th non-zero preamble period in the  $q$ -th band.  $L_q$  is the number of nonzero preamble symbols in the  $q$ -th band and it depends on the preamble pattern and the band index  $q$  (c.f. Fig. 2). Let  $\{x_q(k)\}$  denote the low-pass-equivalent time-domain channel output signal samples corresponding to the  $q$ -th band. Then the corresponding low-pass-equivalent time-domain received samples  $\{r_q(t_l^q(i))\}$  in the  $q$ -th band can be expressed as

$$r_q(t_l^q(i)) = e^{j\varphi} e^{j2\pi v_q t_l^q(i)/N} x_q(t_l^q(i)) + n(t_l^q(i)) \quad (6)$$

where  $v_q$  is the normalized (by the sub-carrier spacing) CFO of the  $q$ -th band,  $\varphi$  is an arbitrary carrier phase,  $\{n(t_l^q(i))\}$  are independent and identically distributed, circularly-symmetric complex Gaussian noise samples with zero mean and variance  $\sigma^2 = E\{|n(t_l^q(i))|^2\}$ .

### III. PROPOSED FREQUENCY OFFSET ESTIMATION

The proposed frequency offset estimation is based on the BLUE principle and the correlation among the received non-zero preamble symbols in the same band. For each preamble pattern, the channel output preamble in each band has identical parts but the channel output preambles in different bands are not the same due to different channel responses. Let  $D_q$  denote

<sup>2</sup>Our proposed estimator can be applied to other implementations of carrier frequencies generation by changing the values in (5) accordingly.

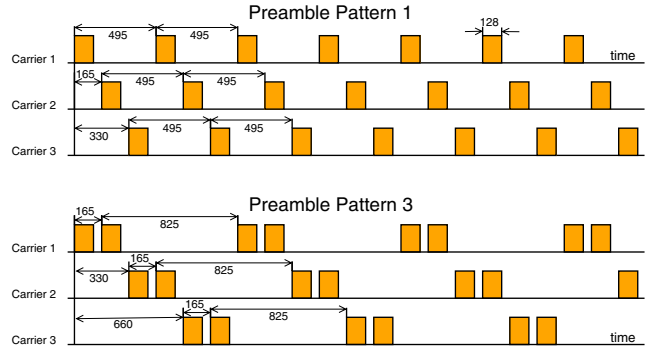


Fig. 2. The preamble structures of [2] in each of the three frequency bands together with their relative distances in samples

the total number of periods counting from the first non-zero preamble period of the  $q$ -th band to the end of the last non-zero preamble period and  $N_q = D_q M_0$ . For the preamble patterns 1 and 2, for example, we have  $D_1 = 20$ ,  $D_2 = 19$ , and  $D_3 = 14$  (see Fig. 2). Define the correlation term with a correlation distance  $d(m)$  between non-zero identical parts of the preamble in the  $q$ -th band as

$$R_q(m) = \sum_{\{k, k+d(m)\} \in \{t_l^q\}} r_q^*(k) r_q(k+d(m)), \quad 1 \leq m \leq H_q \quad (7)$$

where  $H_q$  is a design parameter with  $0 < d(H_q) < N_q$  and  $d(m)$  ( $m = 1, 2, \dots$ ) is an integer multiple of  $M_0$ . For the preamble pattern 1 or 2,  $d(m) = 3mM_0$  in all the three frequency bands, and for the preamble pattern 3 or 4,  $d(m) = 6mM_0$ ,  $(6(m-1)+1)M_0$ , or  $(6m-1)M_0$ . By substituting (6) into (7), we obtain

$$R_q(m) = e^{j2\pi v_q d(m)/N} \{Q_q(m)E_q + G_q(m) + N_q(m)\} \quad (8)$$

$$\text{where } Q_q(m) \triangleq \left\langle \frac{N_q - d(m) - M_0}{d_0} \right\rangle + 1 \quad (9)$$

$$d_0 = \begin{cases} 3M_0, & \text{preamble 1 \& 2} \\ 6M_0, & \text{preamble 3 \& 4} \end{cases} \quad (10)$$

$$E_q \triangleq \sum_{k=0}^{N-1} |x_q(k)|^2 \quad (11)$$

$$G_q(m) \triangleq \sum_{\{k, k+d(m)\} \in \{t_l^q\}} \{x_q^*(k)\tilde{n}(k+d(m)) + x_q(k+d(m))\tilde{n}^*(k)\} \quad (12)$$

$$N_q(m) \triangleq \sum_{\{k, k+d(m)\} \in \{t_l^q\}} \tilde{n}^*(k)\tilde{n}(k+d(m)) \quad (13)$$

$\langle X \rangle$  denotes the integer part of  $X$ .  $\tilde{n}(k) \triangleq n(k)e^{-j2\pi v k/N}$  is a random variable statistically equivalent to  $n(k)$ . Define

$$\theta_q(m) \triangleq \frac{N}{2\pi d(m)} \text{angle}\{R_q(m)\}. \quad (14)$$

If  $|v_q| < N/(2d(m))$ , then we have

$$\theta_q(m) = v_q + \frac{N}{2\pi d(m)} \text{angle}\{Q_q(m)E_q + G_q(m) + N_q(m)\} \quad (15)$$

which gives an estimate of  $v_q$ . Then the frequency offset estimator based on BLUE [10] for the  $q$ -th band is

$$\hat{v}_q = \sum_{m=1}^{H_q} \omega_q(m) \theta_q(m) \quad (16)$$

$$\begin{aligned}
\mathbf{C}_{\theta_q}^{(1,1)}(m, n) &= \frac{N^2 \sigma^2}{4\pi^2 E_q} \frac{1}{d_1(m)d_1(n)Q_{q,1}(m)Q_{q,1}(n)} \\
&\times \begin{cases} 2m + \frac{Q_{q,1}(m)N\sigma^2}{2E_q}, & \text{if } m = n \text{ \& } d_1(m) < \min(N_{q,1}^o, N_{q,1}^e)/2 \\ m + \min(Q_{q,1}^o(m), Q_{q,1}^e(m)) + \frac{Q_{q,1}(m)N\sigma^2}{2E_q}, & \text{if } m = n \text{ \& } \min(N_{q,1}^o, N_{q,1}^e)/2 \leq d_1(m) < \max(N_{q,1}^o, N_{q,1}^e)/2 \\ Q_{q,1}(m) + \frac{Q_{q,1}(m)N\sigma^2}{2E_q}, & \text{if } m = n \text{ \& } d_1(m) \geq \max(N_{q,1}^o, N_{q,1}^e)/2 \\ 2\min(m, n), & \text{if } m \neq n \text{ \& } d_1(m) + d_1(n) < \min(N_{q,1}^o, N_{q,1}^e) \\ \min(m, n) + \min(Q_{q,1}^o(m), Q_{q,1}^e(m), Q_{q,1}^o(n), Q_{q,1}^e(n)), & \text{if } m \neq n \text{ \& } \min(N_{q,1}^o, N_{q,1}^e) \leq d_1(m) + d_1(n) < \max(N_{q,1}^o, N_{q,1}^e) \\ \min(Q_{q,1}^o(m), Q_{q,1}^o(n)) + \min(Q_{q,1}^e(m), Q_{q,1}^e(n)), & \text{if } m \neq n \text{ \& } d_1(m) + d_1(n) \geq \max(N_{q,1}^o, N_{q,1}^e) \end{cases} \quad (28)
\end{aligned}$$

where  $\omega_q(m)$  is the  $m$ -th component of the weighting vector

$$\omega_q = \frac{\mathbf{C}_{\theta_q}^{-1} \mathbf{1}}{\mathbf{1}^T \mathbf{C}_{\theta_q}^{-1} \mathbf{1}} \quad (17)$$

and  $\mathbf{C}_{\theta_q}$  is the covariance matrix of  $\{\theta_q(m) : m = 1, \dots, H_q\}$ .

Next, we combine  $\{\hat{v}_q\}$  from the different frequency bands (c.f. Fig. 1) by using the BLUE principle, together with (4) and (14), and obtain the estimate of  $v$  as

$$\hat{v} = \sum_{q=1}^3 \sum_{m=1}^{H_q} \bar{\omega}_q(m) \theta_q(m) / b_q \quad (18)$$

where the weighting values are given by

$$[\bar{\omega}_1(1), \dots, \bar{\omega}_1(H_1), \dots, \bar{\omega}_3(1), \dots, \bar{\omega}_3(H_3)]^T = \frac{\mathbf{C}^{-1} \mathbf{1}}{\mathbf{1}^T \mathbf{C}^{-1} \mathbf{1}} \quad (19)$$

and  $\mathbf{C}$  is the covariance matrix of  $[\theta_1(1)/b_1, \dots, \theta_1(H_1)/b_1, \theta_2(1)/b_2, \dots, \theta_2(H_2)/b_2, \theta_3(1)/b_3, \dots, \theta_3(H_3)/b_3]$  given by

$$\mathbf{C} = \text{diag} \left\{ \frac{\mathbf{C}_{\theta_1}}{b_1^2}, \frac{\mathbf{C}_{\theta_2}}{b_2^2}, \frac{\mathbf{C}_{\theta_3}}{b_3^2} \right\}. \quad (20)$$

From (16)-(20), we can also express (18) as

$$\hat{v} = \frac{\sum_{q=1}^3 \mathbf{1}^T \mathbf{C}_{\theta_q}^{-1} b_q \hat{v}_q}{\sum_{q=1}^3 \mathbf{1}^T \mathbf{C}_{\theta_q}^{-1} b_q^2}. \quad (21)$$

The covariance matrices required in the above estimation are addressed in the following.

#### A. Method A

Equation (15) can be expressed as

$$\theta_q(m) = v_q + \frac{N}{2\pi d(m)} \tan^{-1}(B(m)) \quad (22)$$

$$B(m) = \frac{\Im\{G_q(m)\} + \Im\{N_q(m)\}}{Q_q(m)E_q + \Re\{G_q(m)\} + \Re\{N_q(m)\}} \quad (23)$$

where  $\Re\{\cdot\}$  and  $\Im\{\cdot\}$  are the real and the imaginary parts of  $\{\cdot\}$ , respectively, and  $\tan^{-1}$  is the four-quadrant arctangent function. For high SNR, we can approximate (22) as

$$\theta_q(m) \simeq v_q + \frac{N}{2\pi d(m)} \frac{\Im\{G_q(m)\} + \Im\{N_q(m)\}}{Q_q(m)E_q}. \quad (24)$$

1) *Preamble Patterns 1 & 2*: The preamble structure in each band is the same and adjacent identical parts have the same distance of  $3M_0$ . So  $d(m) = 3mM_0$  and  $Q_q(m) = (L_q - m)$ . After straight-forward calculation, the  $m$ -th row,  $n$ -th column element of  $\mathbf{C}_{\theta_q}$  can be expressed as

$$\begin{aligned}
\mathbf{C}_{\theta_q}(m, n) &= \frac{N^2 \sigma^2}{4\pi^2 (3M_0)^2 E_q} \frac{1}{mn(L_q - m)(L_q - n)} \\
&\times \begin{cases} m + \frac{(L_q - m)N\sigma^2}{2E_q}, & \text{if } m = n \text{ \& } m < L_q/2 \\ (L_q - m) + \frac{(L_q - m)N\sigma^2}{2E_q}, & \text{if } m = n \text{ \& } m \geq L_q/2 \\ \min(m, n), & \text{if } m \neq n \text{ \& } m + n < L_q \\ L_q - \max(m, n), & \text{if } m \neq n \text{ \& } m + n \geq L_q. \end{cases} \quad (25)
\end{aligned}$$

2) *Preamble Patterns 3 & 4*: All possible correlation distances for the preamble patterns 3 and 4 in all three bands (see Fig. 2) are  $\{M_0, 5M_0, 6M_0, 7M_0, 11M_0, 12M_0, 13M_0, 17M_0, 18M_0, 19M_0\}$  which can be grouped into 3 categories:  $\{d_1(m) = 6mM_0, 1 \leq m \leq H_{q,1}\}$ ,  $\{d_2(m) = (6(m-1) + 1)M_0, 1 \leq m \leq H_{q,2}\}$ , and  $\{d_3(m) = (6m-1)M_0, 1 \leq m \leq H_{q,3}\}$ , where  $H_{q,1}$ ,  $H_{q,2}$ , and  $H_{q,3}$  are design parameters. Let  $D_{q,i}$  denote the total number of periods (including null symbol intervals) of the preamble used to calculate the correlation with the correlation distance  $d_i$  on the  $q$ -th band, counting from the first non-zero preamble period to the end of last non-zero preamble period used in the correlation term.  $D_{q,1}$  is a special case where we separate it into  $D_{q,1}^o$  and  $D_{q,1}^e$ , corresponding to the correlation distance  $6mM_0$  on the odd symbol indices and the even symbol indices, respectively. Then  $N_{q,1}^o = D_{q,1}^o M_0$ ,  $N_{q,1}^e = D_{q,1}^e M_0$ , and  $N_{q,i} = D_{q,i} M_0$  for  $i = 2, 3$ . For the correlation term with a correlation distance  $d_i(m)$ , (24) becomes

$$\theta_{q,i}(m) \simeq v_q + \frac{N}{2\pi d_i(m)} \frac{\Im\{G_{q,i}(m)\} + \Im\{N_{q,i}(m)\}}{Q_{q,i}(m)E_q} \quad (26)$$

where  $Q_{q,i}(m) = \left\langle \frac{N_{q,i} - d_i(m) - M_0}{6M_0} \right\rangle + 1$  for  $i = 2, 3$ ,  $Q_{q,1}(m) = Q_{q,1}^o(m) + Q_{q,1}^e(m)$ , where  $Q_{q,1}^o(m) = \left\langle \frac{N_{q,1}^o - d_1(m) - M_0}{6M_0} \right\rangle + 1$ ,  $Q_{q,1}^e(m) = \left\langle \frac{N_{q,1}^e - d_1(m) - M_0}{6M_0} \right\rangle + 1$ , and  $G_{q,i}(m)$  and  $N_{q,i}(m)$  are the same as  $G_q(m)$  and  $N_q(m)$ , respectively, except that  $d(m)$  is replaced by  $d_i(m)$ . Then the covariance matrix  $\mathbf{C}_{\theta_q}$  can be expressed as

$$\mathbf{C}_{\theta_q} = \begin{bmatrix} \mathbf{C}_{\theta_q}^{(1,1)}, & \mathbf{C}_{\theta_q}^{(1,2)}, & \mathbf{C}_{\theta_q}^{(1,3)} \\ \mathbf{C}_{\theta_q}^{(2,1)}, & \mathbf{C}_{\theta_q}^{(2,2)}, & \mathbf{C}_{\theta_q}^{(2,3)} \\ \mathbf{C}_{\theta_q}^{(3,1)}, & \mathbf{C}_{\theta_q}^{(3,2)}, & \mathbf{C}_{\theta_q}^{(3,3)} \end{bmatrix} \quad (27)$$

where  $\mathbf{C}_{\theta_q}^{(i,l)}$  is the cross-covariance matrix of  $\{\theta_{q,i}(m)\}$  and  $\{\theta_{q,l}(n)\}$ , and elements of  $\mathbf{C}_{\theta_q}^{(i,l)}$  are given by (28)-(31) as

$$\begin{aligned}
\mathbf{C}_{\theta_q}^{(2,3)}(m, n) &= \frac{N^2 \sigma^2}{4\pi^2 E_q} \frac{1}{d_2(m)d_3(n)Q_{q,2}(m)Q_{q,3}(n)} \\
&\times \begin{cases} -\frac{1}{2} \left( \left\langle \frac{N_{q,3}-M_0}{6M_0} \right\rangle + \left\langle \frac{N_{q,2}-M_0}{6M_0} \right\rangle \right) + m + n - 2, & \text{if } d_2(m) + d_3(n) < \min(N_{q,2}, N_{q,3}) \\ -\frac{1}{2} \left( \left\langle \frac{\max(N_{q,2}, N_{q,3}) - M_0}{6M_0} \right\rangle - m - n + 2 \right), & \text{if } \min(N_{q,2}, N_{q,3}) \leq d_2(m) + d_3(n) < \max(N_{q,2}, N_{q,3}) \\ 0, & \text{else.} \end{cases} \quad (31)
\end{aligned}$$

$$\begin{aligned}
\mathbf{C}_{\theta_q}^{(1,1)}(m, n) &= \frac{N^2 \sigma^2}{4\pi^2 E_q} \frac{1}{d_1(m)d_1(n)Q_{q,1}(m)Q_{q,1}(n)} \\
&\times \begin{cases} 2\min(m, n), & \text{if } d_1(m) + d_1(n) < \min(N_{q,1}^o, N_{q,1}^e) \\ \min(m, n) + \min(Q_{q,1}^o(m), Q_{q,1}^e(m), Q_{q,1}^o(n), Q_{q,1}^e(n)), & \text{if } \min(N_{q,1}^o, N_{q,1}^e) \leq d_1(m) + d_1(n) < \max(N_{q,1}^o, N_{q,1}^e) \\ \min(Q_{q,1}^o(m), Q_{q,1}^e(n)) + \min(Q_{q,1}^e(m), Q_{q,1}^o(n)), & \text{if } d_1(m) + d_1(n) \geq \max(N_{q,1}^o, N_{q,1}^e) \end{cases} \quad (34)
\end{aligned}$$

defined below:

$$\begin{aligned}
\mathbf{C}_{\theta_q}^{(1,i)}(m, n)|_{i=2,3} &= \frac{N^2 \sigma^2}{8\pi^2 E_q} \frac{1}{d_1(m)d_i(n)Q_{q,1}(m)Q_{q,i}(n)} \\
&\times \begin{cases} (\min(Q_{q,1}^e(m), Q_{q,i}(n)) \\ + \min(Q_{q,1}^o(m), Q_{q,i}(n))), & \text{if } d_1(m) + d_i(n) \geq N_{q,i} \\ (\min(Q_{q,1}^e(m), Q_{q,i}(n)) + \min(Q_{q,1}^o(m), Q_{q,i}(n)) \\ - 2(Q_{q,i}(n) - m)), & \text{else.} \end{cases} \quad (29)
\end{aligned}$$

$$\begin{aligned}
\mathbf{C}_{\theta_q}^{(i,i)}(m, n)|_{i=2,3} &= \frac{N^2 \sigma^2}{4\pi^2 E_q} \frac{1}{d_i(m)d_i(n)Q_{q,i}(m)Q_{q,i}(n)} \\
&\times \begin{cases} Q_{q,i}(m) + \frac{Q_{q,i}(m)N\sigma^2}{2E_q}, & \text{if } m = n \\ \min(Q_{q,i}(m), Q_{q,i}(n)), & \text{else.} \end{cases} \quad (30)
\end{aligned}$$

Note that  $\mathbf{C}_{\theta_q}$  is Hermitian symmetric.

## B. Method B

Method B uses another high SNR approximation as

$$\theta_q(m) \simeq v + \frac{N}{2\pi d(m)} \frac{\Im\{G_q(m)\}}{Q_q(m)E_q}. \quad (32)$$

After straight-forward calculation using (32),  $\mathbf{C}_{\theta_q}$  can be obtained for the different preamble patterns as follows.

1) *Preamble Patterns 1 & 2*: The  $m$ -th row,  $n$ -th column element of  $\mathbf{C}_{\theta_q}$  can be expressed as

$$\begin{aligned}
\mathbf{C}_{\theta_q}(m, n) &= \frac{N^2 \sigma^2}{4\pi^2 (3M_0)^2 E_q} \frac{1}{mn(L_q - m)(L_q - n)} \\
&\times \begin{cases} \min(m, n), & \text{if } m + n < L_q \\ L_q - \max(m, n), & \text{if } m + n \geq L_q. \end{cases} \quad (33)
\end{aligned}$$

2) *Preamble Patterns 3 & 4*:  $\mathbf{C}_{\theta_q}$  is given by (27) where  $\{\mathbf{C}_{\theta_q}^{(i,l)}(m, n)\}$  for  $i \neq l$  are the same as (29),(31), while those for  $i = l$  are given by (34) and (35):

$$\mathbf{C}_{\theta_q}^{(i,i)}(m, n)|_{i=2,3} = \frac{N^2 \sigma^2}{4\pi^2 E_q} \frac{1}{d_i(m)d_i(n)\max(Q_{q,i}(m), Q_{q,i}(n))}. \quad (35)$$

## C. Design Parameters and Discussions

We can prove that  $\mathbf{C}_{\theta_q}$  gives the minimum BLUE variance in (36) for the maximum size full-rank matrix  $\mathbf{C}_{\theta_q}$ . This fact yields the best design parameters as follows. For Method A, we obtain  $H_q = L_q - 1$  for the preamble patterns 1 and 2, and  $H_{q,1} = \langle (\max(D_{q,1}^o, D_{q,1}^e) - 1)/6 \rangle$ ,  $H_{q,2} = \langle (D_{q,2} + 5)/6 \rangle$ , and  $H_{q,3} = \langle D_{q,3}/6 \rangle$  for the patterns 3 and 4, (i.e.,  $H_q = 6$  for the pattern 1 or 2,  $H_{1,2} = 4$ ,  $H_{1,1} = H_{1,3} = H_{2,1} = H_{2,2} = H_{2,3} = H_{3,2} = 3$ ,  $H_{3,1} = H_{3,3} = 2$  for the pattern 3 or 4). For Method B, we have  $H_q = \langle L_q/2 \rangle$  for the patterns 1 and 2, and  $H_{q,1} =$

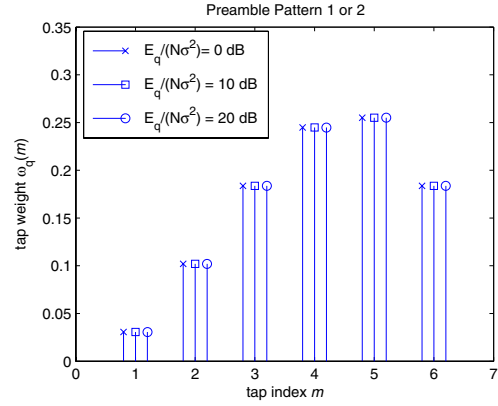


Fig. 3. The robustness of the BLUE weighting values against  $E_q/(N\sigma^2)$

$\langle (\max(D_{q,1}^o, D_{q,1}^e) + 5)/12 \rangle$ ,  $H_{q,2} = \langle (D_{q,2} + 10)/12 \rangle$ ,  $H_{q,3} = \langle (D_{q,3} + 6)/12 \rangle$  for the patterns 3 and 4.

For Method A with the best design parameters mentioned above, the weighting values for each band are insensitive to the  $E_q/(N\sigma^2)$  values of practical interest as shown in Fig. 3<sup>3</sup>. Hence, a fixed design value (say 10) for  $E_q/(N\sigma^2)$  can be used when the weighting values are pre-computed.

Next, we can observe that the covariance matrices  $\{\mathbf{C}_{\theta_q}\}$  are inversely proportional to  $E_q$  and the estimator in (18) or (21) requires the knowledge of  $E_q$ . Here, we can consider two approaches. In the first approach, by assuming that  $\{E_q\}$  are the same for all bands, we can remove the dependence of weighting values on  $E_q$ . In the second approach, we replace  $E_q$  with its estimate  $\hat{E}_q$  which can be obtained by simply averaging the received energies of the non-zero training parts in the  $q$ -th band.

The BLUE variance for the  $q$ -th frequency band is given by

$$\text{Var}\{\hat{v}_q\} = (\mathbf{1}^T \mathbf{C}_{\theta_q}^{-1} \mathbf{1})^{-1} \triangleq \frac{1}{A_q E_q}. \quad (36)$$

Hence, the estimator in (21) can also be interpreted as the weighted average of  $\{\hat{v}_q/b_q\}$  where the weighting values are the inverse of the variance of  $\{\hat{v}_q/b_q\}$ . From (36), the first

<sup>3</sup>Only the results of the preamble pattern 1 or 2 are presented due to space limitation but the robustness also holds for the preamble pattern 3 or 4.

approach (without energy weighting) for (18) is given by

$$\hat{v} = \frac{\sum_{q=1}^3 A_q b_q \hat{v}_q}{\sum_{q=1}^3 A_q b_q^2} \quad (37)$$

and the second approach (with energy weighting) becomes

$$\hat{v} = \frac{\sum_{q=1}^3 \hat{E}_q A_q b_q \hat{v}_q}{\sum_{q=1}^3 \hat{E}_q A_q b_q^2}. \quad (38)$$

In the simulation section, we will evaluate both approaches.

Note that we require  $|v_q| < N/(2d(m))$  to avoid estimation ambiguity in (14). For the correlation terms with large correlation distances  $\{d(m)\}$ , this condition limits the estimation range. This issue can be easily circumvented by performing initial frequency offset compensation on the received preamble signal based on the initial frequency offset estimate obtained from the correlation term(s) with small correlation distance(s). For the preamble pattern 1 or 2, using  $\{R_q(d(1))\}$  for the initial frequency offset compensation will extend the estimation range to  $|\hat{v}_q| < N/(2d(1)) \simeq 0.129$  while the maximum possible carrier frequency offset is  $|v_q|_{\max} = 0.04096b_q$  for the 20 ppm oscillator accuracy specified in [2].

The computational complexities of the proposed methods are relatively low since the methods are based on correlation. The exact complexities in terms of the numbers of equivalent real multiplication (ERM), equivalent real addition (ERA), and the angle operation are presented in Table I for the proposed method without energy weighting<sup>4</sup>. Since the energy estimates  $\{\hat{E}_q\}$  can be obtained from the timing synchronization or automatic gain control stage, additional complexity for the proposed method with energy weighting is minimal.

#### IV. SIMULATION RESULTS

We use the simulation parameters as specified in [2]:  $N = 128$ ,  $N_g = 37$ , carrier frequencies  $f_1 = 3432$  MHz,  $f_2 = 3960$  MHz,  $f_3 = 4224$  MHz, the sub-carrier spacing  $1/T = 4.125$  MHz, and four different preambles. The channel model CM-2 with  $L_h = 6$  and  $K = 6$  is adopted.  $p(t)$  is assumed to be a spectral raised cosine pulse with a filter span of  $[-5T_s, 5T_s]$ . The normalized oscillator frequency offset  $v$  is set to 0.01. The non-zero transmitted preamble samples are normalized to have a unit sample energy. The average channel energy (averaged over the three bands) is set to unity (i.e.,  $(\sum_{q=1}^3 \sum_n |h_q(n)|^2)/3 = 1$ ) and the SNR is defined as  $1/\sigma^2$ . The parameters for the preamble patterns 3 and 4 using Method B are given in Table II. As a reference, we also evaluate the conventional estimators based on correlation and averaging, denoted by ‘‘Cor. ( $i_1, i_2, \dots, i_k$ )’’ in the figures. These estimators are defined by

$$\hat{v} = \frac{1}{3k} \sum_{q=1}^3 \sum_{l=1}^k \theta_q(i_l)/b_q \quad (39)$$

which is simply an average of the estimates  $\theta_q(i_1), \theta_q(i_2), \dots$ , and  $\theta_q(i_k)$  obtained from the correlation terms with correlation distances of  $i_1 M_0, i_2 M_0, \dots$ , and  $i_k M_0$ , respectively.

<sup>4</sup>For example, according to the design parameters mentioned in the subsection C for method A, the numbers of angle operation, ERM, and ERA are, respectively, 18, 32274, and 32237 for preamble patterns 1 and 2, and 26, 32794, and 32741 for preamble patterns 3 and 4.

In Fig. 4 (a) and (b), we present the MSEs of the conventional estimators with different numbers of correlation distances for the preamble patterns 1 (or equivalently 2) and 3 (or equivalently 4), respectively. Using more correlation terms improves the MSE performance at the expense of complexity.

In Figs. 5 and 6, the MSEs of the proposed methods for the preamble patterns 1 (or equivalently 2) and 3 (or equivalently 4), respectively, are presented. Methods A and B with energy weighting (38) are denoted as  $A_E$  and  $B_E$  while those without energy weighting (37) are denoted as  $A$  and  $B$  in the figure. All proposed methods perform better than the conventional estimators. The proposed methods with energy weighting slightly outperform the proposed methods without energy weighting. Method  $A_E$  gives the minimum MSE, which is quite close to the hybrid Cramer-Rao bound (HCRB)<sup>5</sup> [12] at moderate and high SNRs. We also observe that the preamble pattern 1 or 2 gives better MSEs and HCRBs than the preamble pattern 3 or 4. The MSE improvement of the proposed estimators over the conventional estimators is more significant for the preamble patterns 3 and 4. Method  $A_E$  (or  $A$ ) is slightly better than Method  $B_E$  (or  $B$ ) at the expense of additional complexity.

#### V. CONCLUSIONS

We have presented frequency offset estimation methods based on BLUE principle for MB-OFDM based UWB systems. Oscillator frequency mismatch introduces different carrier-frequency offsets in different bands of MB-OFDM systems. The proposed estimators incorporate the effects of different carrier frequency offsets, different channel responses, different channel energies, and different preamble structures in different bands and achieve better performance than the conventional estimators. Preamble patterns 1 and 2 of [2] yield better estimation MSEs and HCRBs than the patterns 3 and 4. Our proposed methods achieve MSEs very close to the HCRBs for moderate to high SNRs and their improvements over the conventional estimators are more significant for the preamble patterns 3 and 4.

#### ACKNOWLEDGMENT

This work is supported in part by the Erik Jonsson School Research Excellence Initiative, the University of Texas at Dallas.

#### REFERENCES

- [1] L. Yang and G. B. Giannakis, ‘‘Ultra-wideband communications: An idea whose time has come,’’ *Signal Processing Magazine, IEEE.*, Vol 21, No. 6, Nov. 2004, pp. 26-54.
- [2] IEEE 802.15 Working Group for Wireless Personal Area Networks (WPANs) ‘‘Multi-band OFDM Physical Layer Proposal for IEEE 802.15 Task Group 3a,’’ Mar. 2004.
- [3] A. Batra, J. Balakrishnan, G. R. Aiello, J. R. Foerster, A. Dabak, ‘‘Design of a multiband OFDM system for realistic UWB channel environments,’’ *IEEE Trans. Microwave Theory and Tech.*, Sept. 2004, pp. 2123-2137.
- [4] P. H. Moose, ‘‘A technique for orthogonal frequency division multiplexing frequency offset correction,’’ *IEEE Trans. Commun.*, Oct. 1994, pp. 2908-2914.

<sup>5</sup>For simplicity in calculating the HCRB, we use a multipath Rayleigh fading channel with a similar power delay profile.

TABLE I  
COMPUTATIONAL COMPLEXITIES OF THE PROPOSED METHODS

	Preamble Pattern 1 or 2	Preamble Pattern 3 or 4
# ERM	$\sum_{q=1}^3 \{4NL_qH_q - 2NH_q(H_q + 1) + H_q\}$	$4N \cdot \sum_{q=1}^3 \sum_{i=1}^3 \sum_{m=1}^{H_{q,i}} \{Q_{q,i}(m)\} + \sum_{q=1}^3 \sum_{i=1}^3 \{H_{q,i}\}$
# ERA	$\sum_{q=1}^3 \{4NL_qH_q - 2NH_q(H_q + 1) - H_q\} - 1$	$4N \cdot \sum_{q=1}^3 \sum_{i=1}^3 \sum_{m=1}^{H_{q,i}} \{Q_{q,i}(m)\} - \sum_{q=1}^3 \sum_{i=1}^3 \{H_{q,i}\} - 1$
# angle{.}	$\sum_{q=1}^3 \{H_q\}$	$\sum_{q=1}^3 \sum_{i=1}^3 \{H_{q,i}\}$

TABLE II  
SIMULATION PARAMETERS FOR PREAMBLE PATTERN 3 OR 4 USING METHOD B

$q$	$D_{q,1}^o, D_{q,1}^e, D_{q,2}, D_{q,3}$	$N_{q,1}^o, N_{q,1}^e, N_{q,2}, N_{q,3}$	$H_{q,1}^o, H_{q,1}^e, H_{q,2}, H_{q,3}$
1	19, 20, 20, 19	$19M_0, 20M_0, 20M_0, 19M_0$	2, 2, 2, 2
2	19, 14, 14, 19	$19M_0, 14M_0, 14M_0, 19M_0$	2, 1, 2, 2
3	13, 14, 14, 13	$13M_0, 14M_0, 14M_0, 13M_0$	1, 1, 2, 1

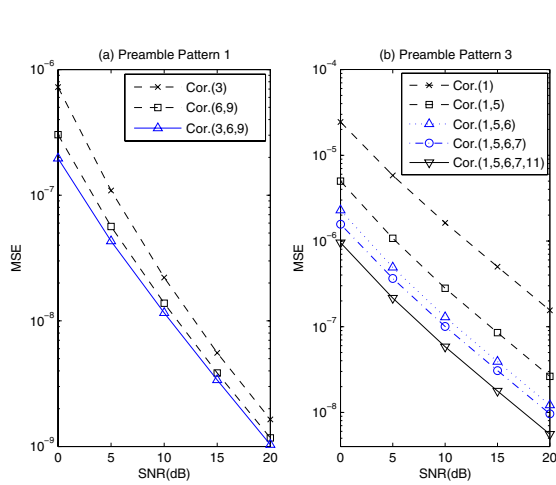


Fig. 4. The normalized frequency offset estimation performance of the conventional method with different numbers of correlation distances

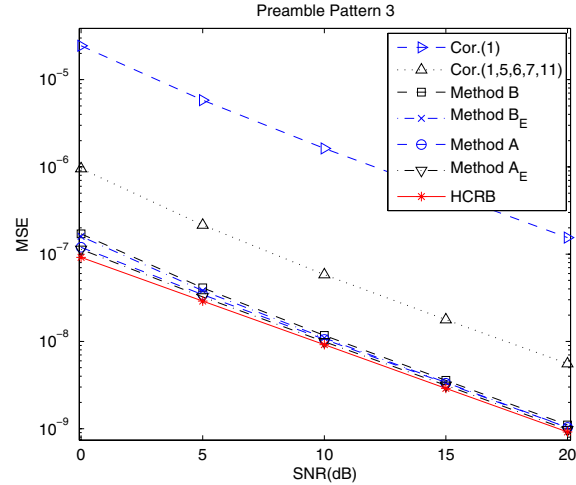


Fig. 6. The normalized frequency offset estimation performance comparison of our proposed methods and the conventional method for the preamble pattern 3 (or equivalently 4)

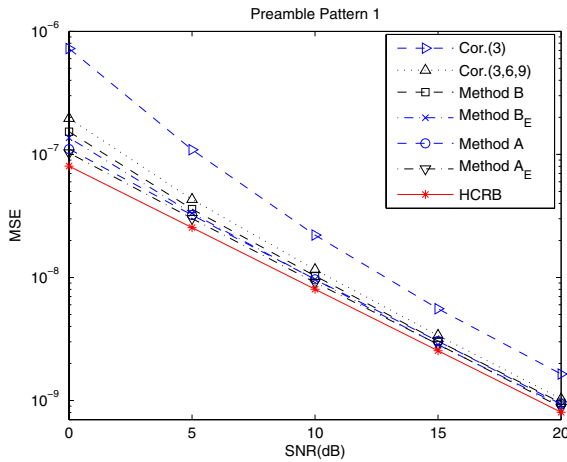


Fig. 5. The normalized frequency offset estimation performance comparison of our proposed methods and the conventional method for the preamble pattern 1 (or equivalently 2)

- [5] T. M. Schmidl and D. C. Cox, "Robust frequency and timing synchronization for OFDM," *IEEE Trans. Commun.*, Dec. 1997, pp. 1614-1621.
- [6] M. Morelli and U. Mengali, "An improved frequency offset estimator for OFDM applications," *IEEE Commun. Letters*, Mar. 1999, pp. 75-77.
- [7] H. Minn, P. Tarasak, V. K. Bhargava, "OFDM frequency offset estimation based on BLUE principle," *IEEE VTC 2002*, pp. 1230-1234.
- [8] H. Minn, P. Tarasak and V. K. Bhargava, "Some issues of complexity and training symbol design for OFDM frequency offset estimation methods based on BLUE principle", *IEEE VTC'03* (Spring), pp. 1288-1292.
- [9] H. Minn and P. Tarasak, "Improved maximum likelihood frequency offset estimation based on likelihood metric design," *ICC*, 2005, pp. 2150-2156.
- [10] S. M. Kay, "Fundamentals of Statistical Signal Processing: Estimation Theory," *Prentice Hall PTR*, 1993.
- [11] A. F. Molisch, J. R. Foerster, M. Pendergrass, "Channel models for Ultrawideband personal area networks," *IEEE Wireless Communications*, Vol. 10, No. 6, pp. 14-21, Dec. 2003.
- [12] H. L. Van Trees, "Optimum Array Processing," *Wiley Interscience*, New York, 2002.